Available online at www.sciencedirect.com
SCIENCE DIRECT®
Journal of Chromatography B, 803 (2004) 67–73
JOURNAL OF CHROMATOGRAPHY B
www.elsevier.com/locate/chromb

Structure–function study of a chlorotoxin-chimer and its activity on Kv1.3 channels

Isabelle Huys [a], Etienne Waelkens [b], Jan Tytgat [a,*]

[a] *Laboratory of Toxicology, Faculteit Farmaceutische Wetenschappen, Katholieke Universiteit Leuven, E. Van Evenstraat 4, 3000 Leuven, Belgium*
[b] *Afdeling Biochemie, Faculteit Geneeskunde, Katholieke Universiteit Leuven, Leuven, Belgium*

Abstract

Chlorotoxin has been isolated from the venom of the scorpion *Leiurus quinquestriatus* and characterized as a 4.1 kDa peptide, containing a lysine at position 27 that is also present in many Kv-blocking toxins. Because chlorotoxin shows no affinity for Kv-channels, we intended to design, express and purify a chlorotoxin-chimer, containing the active binding site (β-sheet) of a very potent Kv1-channel blocking peptide, agitoxin 2, by mutating three original residues in the chlorotoxin molecule. Several derivatives of the chimer, gradually missing one additional amino acid residue at the N-terminal side of the peptide, were produced and identified chromatographically. In contrast to chlorotoxin, these chimer derivatives are capable of blocking cloned Kv1-channels.

Keywords: Structure–function study; Kv1.3 channels; Chlorotoxin-chimer

1. Introduction

Previously, it has been reported that the crude venom, extracted from the scorpion *Leiurus quinquestriatus quinquestriatus* (*Lqq*) inhibits reconstituted small-conductance Cl^- channels isolated from rat epithelia and embryonic rat brain, when applied to the cytoplasmic surface [1]. The active component, chlorotoxin (ClTx, sITx8), has been isolated and characterized as a 4070 Da basic peptide with considerable sequence homology to the class of small insectotoxins [2,3]. Ullrich et al. reported a ClTx-sensitive Cl^- current, present in human astrocytoma cell lines [4]. From then, ClTx has been widely used as a Cl^--channel blocker to analyze Cl^- channels [5–7] and has been proposed as glioma-specific marker with diagnostic and therapeutic potential [8]. Because it is very unlikely that the real natural target of ClTx is located at the intracellular site of the cell membrane, we were interested in other possible interaction sites or ion channels at the extracellular membrane face. Interestingly, when analyzing the primary structure, a lysine at position 27, known to be a crucial residue in the interaction of toxins with the pore of voltage-activated K^+ channels, is present in ClTx. Furthermore, the three-dimensional structure of ClTx seems to consist of an α-helix bound by two disulfide bridges to the second strand of the antiparallel β-sheet and a third disulfide bridge connecting the N-terminus and the C-terminal part of the peptide, the latter structure playing a stabilizing role in other short scorpion toxins [9]. This scaffold is similar to that of α-K^+ channel toxins [10], named α-KTx peptides, which are short-chain scorpion toxins known to block K^+ channels [11]. Most of them have a highly conserved C-terminal region (β-sheet) that is directly involved in K^+ channel interaction. In addition, ClTx has a fourth disulfide bridge. This is not unusual. Although most α-KTx peptides consist of three disulfide bridges, several of these toxins contain four bridges. However, despite the structural similarities, up to now, block of voltage-gated K^+ channels by ClTx has never been shown so far.

For this reason, the aim of our study was to construct a ClTx chimer, with an altered β-sheet, taking the β-sheet of agitoxin 2 as a template for the introduced modifications (Fig. 1). Three amino acids composing the β-sheet in agitoxin 2 (AgTx2), known to be a very potent Kv-channel blocker from the venom of the scorpion *Lqq* [12], were put in place of the corresponding three amino acids in ClTx (ClTx-$GRGKCI_{24–29}$ → $RFGKCM_{24–29}$).

* Corresponding author. Tel.: +32-16-32-34-03; fax: +32-16-32-34-05.
E-mail address: jan.tytgat@pharm.kuleuven.ac.be (J. Tytgat).
URL: http://www.toxicology.be.

1570-0232/$ – see front matter © 2003 Elsevier B.V. All rights reserved.
doi:10.1016/j.jchromb.2003.11.029

Fig. 1. Amino acid sequence comparison. Amino acid sequences of chlorotoxin (ClTx) and agitoxin 2 (AgTx2) were aligned and the relation with the ClTx chimer is shown. Three residues were mutated in ClTx. The arrows on the top of the sequences indicate approximate positions for the β-sheet structure, whereas the rectangle indicates the segment of primary structure involved in the α-helix formation of the three-dimensional structure of the toxins.

2. Experimental

2.1. Solvents, solutions and materials

Tris–HCl, NaCl, $CaCl_2$, Na_2EDTA, maltose, glucose, leupeptine and acetonitrile LiChroSolv (gradient grade for high-performance liquid chromatography, HPLC) were from Merck Eurolabs (Leuven, Belgium). All buffers were freshly prepared using demineralized water from Seralpur Pro90 CN (Ransbach-Baumbach, Germany). Factor Xa (fXa) was from different sources like Boehringer (Brussels, Belgium), Sigma (Bornem, Belgium), New England Biolabs (Beverly, MA, USA). Trifluoroacetic acid (TFA), isopropyl-1-thio-β-galactopyranoside (IPTG), collagenase and tricaine were from Sigma (Bornem, Belgium). Commercially available ClTx was from Latoxan® (Valence, France). All enzymes, the pMAL-p2X vector and the amylose affinity resin were from New England Biolabs (Beverly, MA, USA). The cap analogue diguanosine triphosphate was from Promega (Madison, WI, USA). The T7 mMESSAGE mMACHINE transcription kit was from Ambion (Woodward Austin, TX, USA). The oligonucleotides 5′ ATGTGCATGCCGTGCTTCACGACGGACCACCAGATGGCCCGCAAGTGCGACGA C 3′, 5′ TGCTGCGGCGGCAAGCGCTTCGGGAAGTGCATGGGGCCGCAGTGCCTGTG CCGCTGAG 3′, 5′ TACACGTACGGCACGAAGTGCTGCCTGGTGGTCTACCGGGGCGTTCACGCTGCTGACGACGCCGCCG 3′ and 5′ TTCGCGAAGCCCTTCACGTACCCCGGCGTCACGGACACGGCGACTCCTA 3′ were chemically synthesized on an Applied Biosystem device from Amersham Pharmacia Biotech (Roosendaal, The Netherlands). Genes were extracted from gels using the QIAGEN kit from QIAGEN (AE Leusden, The Netherlands). Capillary needles (Picotip type: EconoTip) for nanospray mass spectrometry were from New Objective (Ringoes, NY, USA). For agarose gel electrophoresis, the DNA marker was from Eurogentec (Ivoz-Ramet, Belgium). The TAE buffer for electrophoresis consisted of 1 M Tris, 15 mM EDTA, 125 mM NaOAc, pH 7.8. The column buffer for affinity chromatography contained 20 mM Tris–HCl, 200 mM NaCl, 1 mM Na_2EDTA, pH 7.4. The ND-96 solution, used in the electrophysiological experiments, contained 96 mM NaCl, 2 mM KCl, 1.8 mM $CaCl_2$, 1 mM $MgCl_2$ and 5 mM HEPES, supplemented with 50 mg/l gentamycin sulfate from Schering-Plough (Kenilworth, NY, USA), only for incubation, and adjusted to pH 7.5. The zero-calcium ND-96 solution was identical to the ND-96 solution without $CaCl_2$.

2.2. Instrumentation

Chromatographic purifications were performed using a SMART® System instrumentation and software from Pharmacia Biotech (Uppsala, Sweden). A μPrecision Pump, a μFraction Collector and a μPeak Monitor were used. For reversed-phase HPLC, a reversed-phase μRPC C_2/C_{18} column from Pharmacia Biotech (Uppsala, Sweden) (300 Å pore size silica; 5 μm particle size, 2.1 mm i.d. × 10 cm length), a reversed-phase C_4 column from Vydac (Vydac 214TP104) (Hesperia, CA, USA) (300 Å pore size silica; 5 μm particle size, 4.6 mm i.d. × 250 mm length) and a reversed-phase C_{18} column from Vydac (Vydac 238TP54) (Hesperia, CA, USA) (monomeric C_{18}, 300 Å pore size silica; 5 μm particle size; 4.6 mm i.d. × 250 mm length) were used. For gel filtration, a Superdex® Peptide PC column from Pharmacia Biotech (Uppsala, Sweden) (3.2 mm i.d. × 30 cm length) was used. The UV absorbance spectrophotometer lambda 16 was from Perkin-Elmer (Wellesly, MA, Belgium). The Matrix-assisted laser desorption ionization (MALDI)-time-of-flight (TOF)-mass spectrometry (MS) was performed on a VG Tofspec from Micromass (Manchester, UK) equipped with a N_2-laser (337 nm). Electrospray ionization (ESI) mass spectrometry was performed on a Perkin-Elmer SCIEX API-3000 triple quadrupole mass spectrometer. Samples were dried using the Speed Vac® Plus, Savant, Life Science International (Minnesota, USA). For electrophysiologic measurements, we used the two-microelectrode voltage clamp system (GeneClamp 500) from Axon Instruments (Burlingham, USA).

2.3. Gene design and expression of recombinant proteins

A DNA sequence encoding the ClTx chimer was designed. The gene was constructed from two overlapping oligonucleotide pairs, each consisting of 54–58 base pairs. Each oligonucleotide was gel-purified and phosphorylated. After annealing and ligation using T4 DNA ligase, the chimer-gene was inserted into the pMAL-p2X vector into the flanking sites of *Xmn*I and *Bam*HI. After cloning into

E. coli DH5α cells, positive clones were detected by restriction analysis of their plasmids. Plasmids were checked on an agarose gel electrophoresis system. DNA was diluted 1:2 with loading dye (bromophenol blue 0.25% and sucrose 40%) and gels were prepared with a TAE buffer. Electrophoresis was performed at 100 V for 20–30 min. DNA bands were visualized using UV light. Plasmids containing the ClTx chimers were multiplied using *E. coli* strain DH5α.

The *E. coli* strain DH5α harboring the pMAL-p2X plasmids, was cultured and induced with IPTG and the maltose-binding protein (MBP)-fusion protein was purified by affinity chromatography as described previously [13]. The extinction coefficient for the fusion protein (at 280 nm) was 1.47 (for concentration of 1 mg/ml). The fusion protein was cleaved from the toxin with fXa in different conditions (see Section 3).

2.4. Conditions for purification of recombinant fusion proteins

2.4.1. Affinity chromatography

The periplasmic extracts (400 ml) were loaded onto a column (1.5 cm × 23 cm), filled with amylose affinity resin, at a flow rate of 1 ml/min in column buffer. After washing off the unbound proteins, the bound MBP-fusion proteins were eluted from the amylose resin using the same column buffer containing 10 mM maltose. Twenty fractions of 3 ml each were collected and the fusion protein was detected by the UV absorbance spectrophotometer at 280 nm.

2.4.2. Gel filtration and column calibration

The protein-containing fractions were pooled and further purified using a Superdex® Peptide gel filtration column on the SMART® System. The elution was performed with a buffer containing 20 mM Tris–HCl and 100 mM NaCl, pH 8.0. Controls were performed with cells containing no vector or cells containing the vector without insert.

The solute behavior on our gel filtration column has been characterized using the following formula: $K_{av} = (V_e - V_o)/(V_t - V_o)$, with K_{av} the coefficient defining the proportions of the pores occupied by the solutes, V_e the elution volume, V_o the void volume (40 ml), and V_t the total packed bed volume (96.6 ml). For calibration, three standards were used: cytochrome *c* (horse heart: approx. molecular weight 12.400 Da), aprotinin (bovine lung: approx. weight 6.500 Da) and insulin chain B oxidized (bovine insulin: approx. weight 4.050 Da). Based on a constructed calibration curve, the molecular weight of the protein-containing fractions could be calculated.

2.4.3. High-performance liquid chromatography (HPLC)

The peptide fraction from the gel filtration step was applied onto a 214TP104 C_4 reversed-phase HPLC column and equilibrated with 0.1% TFA at 25 °C to check the purity of the sample. After 5.5 min, a linear gradient has been applied for 24.5 min from 0 to 50% acetonitrile. The flow rate was 0.75 ml/min and absorbance was measured by 214, 254 and 280 nm.

2.5. Conditions for purification and identification of recombinant toxins

The enzymatic cleavage of the pooled fusion proteins, to release the toxin molecule, was carried out at various conditions by fX_a (different sources, see Section 2.1).

2.5.1. High-performance liquid chromatography

Separations of the recombinant proteins were first performed with a 218TP104 C_{18} reversed-phase HPLC column equilibrated with 0.1% TFA at 25 °C. After 4 min an immediate step to 5% acetonitrile (with 0.1% TFA) was followed by a linear gradient to 30% acetonitrile for 5 min and consequently by a linear gradient to 60% for the last 12 min. The flow rate was 0.75 ml/min and the absorbance was simultaneously measured at 214, 254 and 280 nm. The fraction containing the recombinant toxin was recovered and applied on a μRPC C_2/C_{18} SC 2.1/10 reversed-phase HPLC column. After 2.5 min, a linear gradient of acetonitrile was applied for 14 min to 20%, followed by a gradient up to 30% for 1 min, an isocratic gradient for the next 1 min and a decreasing gradient to 0% for the last 1 min. The flow rate was 0.2 ml/min. The toxin was collected and dried. Commercially available ClTx was checked for purity by reversed-phase C_{18} HPCL, in similar conditions as described above. Based on the law of Lambert–Beer, the concentration of this sample could be calculated and compared with the indicated amount of the purchased ClTx.

2.5.2. Matrix-assisted laser desorption ionization (MALDI)-time-of-flight (TOF)-mass spectrometry (MS)

For mass examination, 1 pmol of the sample was dried and redissolved in 0.1% TFA in acetonitrile. This sample was mixed with an equal volume of matrix solution (50 mM α-cyano-4-hydroxy-cinnamic acid in 50:50 (v/v) ethanol/acetonitrile) and loaded on a stainless steel target plate. The molecular mass was determined with a MALDI-TOF mass spectrophotometer operating in the linear and in the reflectron mode.

2.5.3. Electrospray ionization MS

The toxin was dissolved in 0.5% formic acid/50% acetonitrile in HPLC grade water. One microliter was loaded in an EconoTip, a borosilicate capillary needle for static nanospray, and analyzed on a triple quadrupole mass spectrometer equipped with a Protana NanoES source from Protana Engineering (Odense M, Denmark). The sample was sprayed at a flow rate of 30–50 nl/ml. The observed masses were compared with theoretical peptide fragment ion masses.

2.6. Functional characterization

Kv1.3 (*human*) [14]: Plasmids pCI.neo containing the gene for Kv1.3 were linearized with *Not*I and in vitro transcribed using the large-scale T7 mMESSAGE mMACHINE transcription kit.

Stage V–VI *Xenopus laevis* oocytes were isolated by partial ovariectomy under anesthesia (tricaine, 1 g/l). Anaesthetized animals were kept on ice during dissection. The oocytes were defolliculated by treatment with 2 mg/ml collagenase in zero-calcium ND-96 solution. Between 2 and 24 h after defolliculation, oocytes were injected with 50 nl of 1–100 ng/μl cRNA. To stop defolliculation, oocytes are repeatedly washed with zero-calcium ND-96 solution and ND-96 solution to remove all detritus and collagenase. The oocytes were then incubated in ND-96 solution at 18 °C for 1–4 days. Whole-cell currents from oocytes were recorded 1–4 days after injection, using the two-microelectrode voltage clamp technique. Voltage and current electrodes (0.4–2 MΩ) were filled with 3 M KCl. Current records were sampled at 0.5 ms intervals after low pass filtering at 1 kHz. Off-line analysis was performed on a Pentium(r) III processor computer. The recording chamber (100 μl) was constantly perfused and the bath solution was ND-96. All experiments were performed at room temperature (19–23 °C).

3. Results

3.1. Agarose gel electrophoresis patterns of the transformants

Plasmids containing the correct gene were checked using a 1% agarose gel electrophoresis system. Two positive clones were detected and further analyzed.

3.2. Recombinant expression of chlorotoxin-chimer

The fusion protein of the chimer has successfully been expressed in DH5α cells, as described in Section 2. Different conditions for induction were used, varying the induction temperature from 37 to 42 °C, the amount of IPTG from 0.2 to 0.5 mM final concentration and the induction time from 2 to 4 h. Optimal induction conditions for this specific protein were obtained following an induction at 37 °C for 3.5 h using 0.3 mM IPTG (final concentration). Glucose (2 g/l culture) was added into the cell growth medium to repress the maltose genes on the DNA of the *E. coli* host cells, because one of these genes encodes an amylase which can degrade the amylose on the affinity resin (see Section 3.2). Regarding the preparation of the periplasmic extracts using the osmotic shock process, soluble fusion proteins were stable at room temperature when using ice-cold aqueous buffers.

3.3. Purification and cleavage of fusion proteins

The use of the amylose affinity column for initial capture of the fusion protein from the periplasmic extract was an integral part of the purification strategy. Fusion proteins were immobilized to the column and purified from other cell components by supplementing the column buffer. No fusion protein molecules could be detected in the flow-through of the column buffer. Columns held at low temperature (0–4 °C) gave the highest yield of intact fusion proteins. Initially, a small-scale experiment was carried out to determine the behavior of our recombinant fusion protein and to determine the optimal conditions. Using the amylose affinity chromatography, we make use of the specific interaction between the maltose-binding protein group of the fusion protein and the amylose side chains on the column. To visualize, UV spectra were recorded for each 3 ml fraction. Each time, the second fraction showed the presence of a protein, absorbing at 280 nm. The amount of amylose resin needed to purify the fusion protein depends on the amount of fusion protein produced. We tried several conditions, and found that 3 mg/ml bed volume was sufficient for a yield of 30.98 ± 1.72 mg fusion protein per liter cell culture. To concentrate and further clean-up the sample from other cell contaminants, two different methods were used: gel filtration and HPLC. When the samples were applied on the gel filtration column, the detected curve presented one symmetric band at 65 min. No additional peaks were detected and no oligomers were formed. The fusion protein was eluted on the column using a buffer specific for fXa, making an additional lyophilization or drying step unnecessary. In parallel, fusion proteins were applied onto a C_4 reversed-phase HPLC column. We used this type of column because the large size of the fusion protein (about 48 kDa). The protein-containing fraction eluting at 27 min was collected and dried. Fusion proteins were redissolved in the specific fXa buffer for further cleavage.

3.4. Cleavage of fusion proteins using fXa

Optimal conditions for cleavage were performed with 0.5 U fXa/μg fusion protein, in a buffer containing 20 mM Tris–HCl pH 8.0, 100 mM NaCl and 2 mM $CaCl_2$. All other conditions did not result in any cleaved protein fraction. We also tried to cleave the fusion proteins when bound to the amylose resin, but no good results were obtained. Two problems make this method less ideal. First, it requires a lot of fXa. Second, this method is very time consuming (more than 48 h) and some of the fusion proteins may elute from the column during this time, as could be detected by HPLC.

3.5. Purification and identification of recombinant proteins

The fXa digests, supposed to contain small peptides with an expected mass below 5 kDa, were applied onto a monomeric C_{18}-reversed-phase HPLC column (prepared by bonding hydrocarbon chlorosilanes with one reactive chlorine to the silica matrix) (Fig. 2A), resulting in different peaks. All fractions were collected and screened for activity on Kv1-type channels, heterologously expressed in *X. laevis*

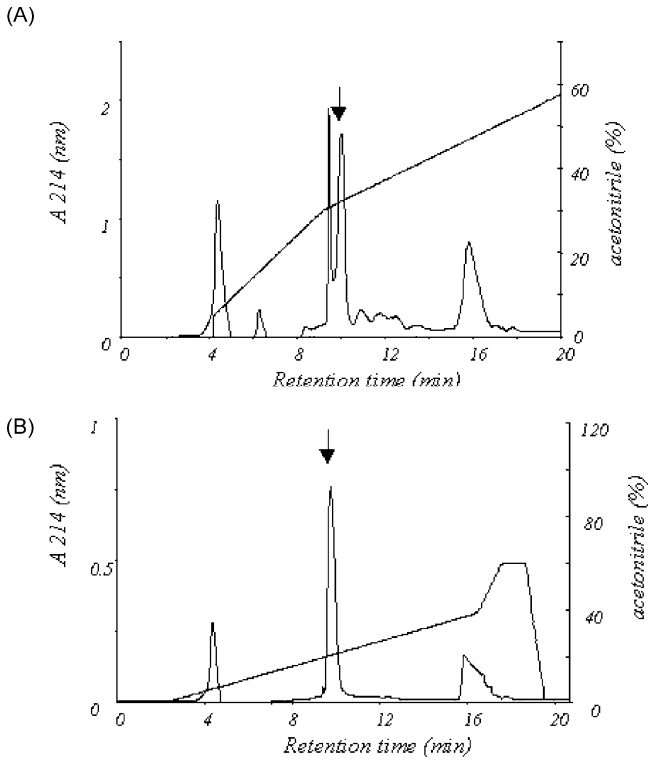

Fig. 2. Purification of recombinant peptides. (A) The restriction digests were applied on a reversed-phase C_{18} HPLC column and all different peaks were tested for activity. (B) The active peak indicated by the arrow in A was further purified on a reversed-phase C_2/C_{18} HPLC column.

oocytes. Fig. 3 shows that the fraction eluting from the C_{18} column at 32% acetonitrile inhibits currents through Kv1.3 channels. The same figure shows that 60 pM rAgTx2 (produced by the same pMAL-p2X strategy) inhibited Kv1.3 currents by 50%, whereas 25 μM WT ClTx did not effect these K^+ currents.

In a next step, the active fraction has been submitted to a C_2/C_{18} reversed-phase HPLC column (Fig. 2B), using a more shallow gradient. This separation resulted in one single peak, eluting at 20% acetonitrile. Studies on Kv1-type channels revealed the presence of a high-affinity peptide in the sample (Fig. 3A).

The molecular mass of this active fraction has been checked by MALDI-TOF MS and ESI nanospray MS on a triple quadrupole mass spectrometer. Surprisingly, different peptide masses were obtained: 2408, 2565, 2636, 2767, 2895 and 3032 Da. Moreover, no mass could be detected that correlates with the intact ClTx chimer (4063 Da). All these peptides eluted at an identical position in the HPLC purification steps, when using different columns (C_2/C_{18}, C_{18}, C_4), as shown for the C_2/C_{18} column (Fig. 2A) and C_{18} column (Fig. 2B). Therefore, we could not separate the molecules in order to identify their individual functional activities. We can not exclude that other methods, like ion exchange chromatography or other reversed-phase packings, can separate the individual fractions.

Using a custom designed program (made by Prof. E. Waelkens), the molecular masses of the fragments were compared with the theoretical ClTx-chimer protein mass and sequence. These masses correlated to the amino acid sequences of peptide fragments derived from the ClTx-chimer protein (Fig. 4). The largest fragment (3032 Da) represented the C-terminal part of the ClTx chimer, lacking the first 9 N-terminal residues (Fig. 5D). All other peptide fragments gradually missed one additional N-terminal amino acid residue. Fig. 5 presents the structure of chlorotoxin and the homology models for the theoretical intact ClTx chimer and chimer derivatives.

4. Discussion

In this work, we used analytical purification procedures to separate peptides from different origins (periplasmic extracts, protein digests). Both large recombinant fusion

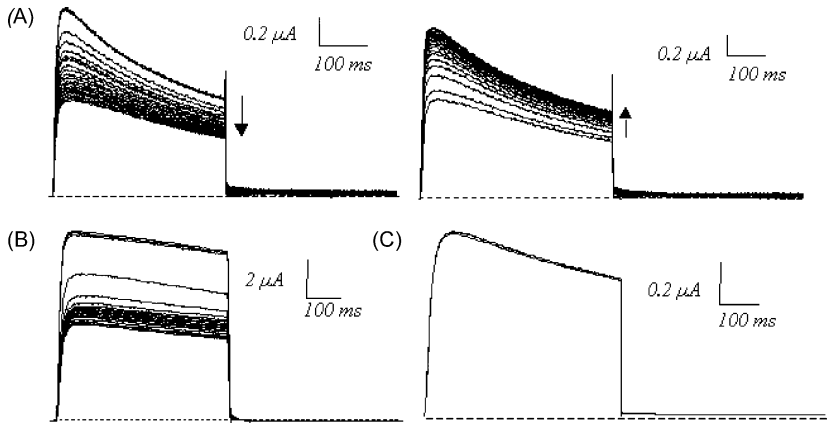

Fig. 3. Electrophysiological effects of the active fraction. Whole cell K^+ currents through Kv1.3 channels, expressed in *Xenopus* oocytes, are evoked by depolarizing the oocytes from a holding potential of −90 to 0 mV for 500 ms. The pulse interval was 1 s. Oocytes were clamped back to −90 mV. (A) Wash-in and wash-out of the ClTx-chimer fraction mix on Kv1.3 channels. Currents were reversibly blocked up to 50%. (B) Effect of 60 pM rAgTx2 on Kv1.3 channels. (C) No inhibition of Kv1.3 currents could be observed in the presence of 25 μM WT ClTx.

Fragments	$MW_{detected}$ (Da)	$MW_{calc.}$ (Da)
MCMP C FTTDHQMARK C DD C C GGKRFGK C MGPQ C L C R	4062.95	4063
HQMARK C DD C C GGKRFGK C MGPQ C L C R	3032.67	3033
QMARK C DD C C GGKRFGK C MGPQ C L C R	2895.53	2895
MARK C DD C C GGKRFGK C MGPQ C L C R	2767.39	2767
ARK C DD C C GGKRFGK C MGPQ C L C R	2636.2	2636
RK C DD C C GGKRFGK C MGPQ C L C R	2565.12	2565
K C DD C C GGKRFGK C MGPQ C L C R	**2408.93**	**2409**

Fig. 4. Alignment of the CTB fragments. Six different consecutive fragments were produced, differing each by only one N-terminal amino acid residue.

proteins and peptide fragments from enzymatic digests could be purified in milligram quantities for further cleavage (MBP) or microquantities for subsequent sequencing (recombinant toxins).

The aim of our study was to produce a ClTx chimer that, in contrast to WT ClTx, displays K^+ channel blocking activity. The fact that ClTx adopts a similar conserved and well-ordered α/β structure, supported our intention to graft a new function onto this structural scaffold, as has previously been performed using other toxin molecules [15–17]. But instead of producing a four-disulfide bridge folded ClTx chimer, six different fragments were formed with only six cysteine residues. Although the specific pattern of the disulfide bridge folding in these fragments has not been determined yet, it has been shown, by NMR studies, for other scorpion toxin analogs (like the analogs of leiurotoxin I) that the absence of the first disulfide bridge does not affect the three-dimensional folding of the toxin molecule, nor it affects the bioactive conformation of the toxin [18,19]. The analogs were fully active in vitro on ion channels and in vivo when tested for neurotoxicity in mice [20]. Similarly, charybdotoxin (ChTx) analogs, lacking the first disulfide bridge, preserve the ability to form native disulfide pairings, in contrast to analogs lacking the second or third bridge [21]. On the other hand, studies on mono-loop analogues of iberiotoxin (IbTx) indicated that no single loop derivative displayed biological activity [22]. Therefore, the observed activity of the fragment mix is most likely similar to the activity of the full ClTx chimer and relays on the correct formation of at least two or three disulfide bridges in the fragments, thereby preserving the conserved α/β core motif in scorpion toxin molecules, also found in insect defensins [23], plant γ-thionins [24], in a sweet tasting protein [25] and in a family of protease inhibitors

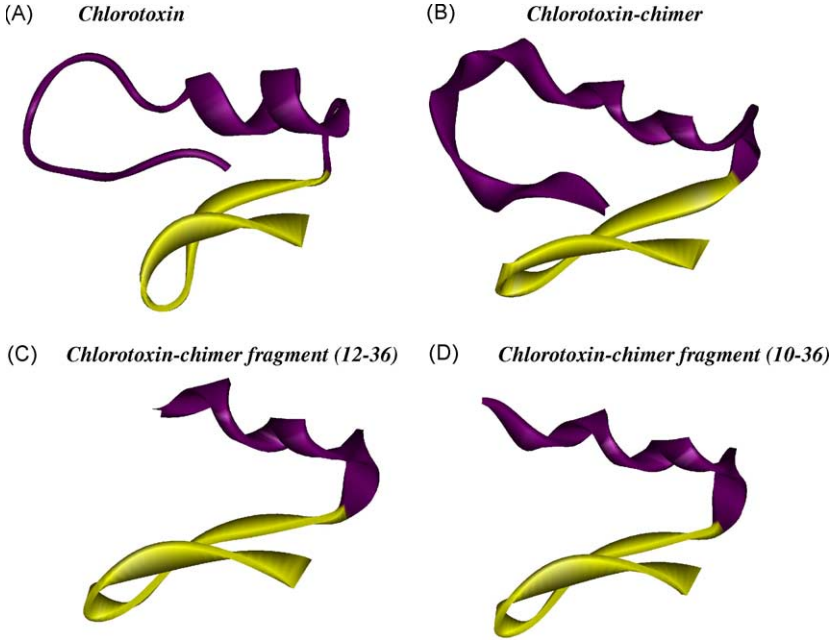

Fig. 5. Homology modeling. (A) Structure of WT ClTx (accession number P45639), (B) structural model of intact ClTx chimer, and structural models for the fragments missing 11 N-terminal residues (C) and 9 N-terminal residues (D). For the models, initial backbone fitting and energy minimization steps were performed with the DeepView program (http://www.expasy.ch/spdbv) and further refined via submission to the Swiss-Model server (http://www.expasy.ch/swissmod/SWISS-MODEL.html).

[26]. Additional experiments are needed in which the individual fragments are recombinantly expressed to verify this observation.

The N-terminal breakdown observed with the ClTx chimer was completely unexpected. In an attempt to overcome the problem of this degradation, we changed different parameters in the purification process of the expressed molecules. For instance, we added leupeptine as a protease inhibitor, we increased the concentration of EDTA from 0.5 to 1.3 mM in the buffer solutions and carried out all experiments at very low temperatures (0–4 °C). However, in contrast to other scorpion toxins with three disulfide bridges that can be expressed very well using the same strategy [13,27], no full-length ClTx chimer could be produced. It seems that the lack of four-disulfide bridges in the ClTx chimer results in a very unstable protein. An attractive idea is that the missing first disulfide bridge only stabilizes the structure of the toxin, without influencing the folding process, as shown for ClTx [9,20]. The lack of the N-terminal part of our ClTx chimer can therefore be linked to the lack of stability. The ClTx chimer will be unstable and N-terminal residues may be removed. The stabilizing action of a disulfide bridge is in agreement with the observation that the N-terminal degradation indeed stops at Lys17, the position preceding the first possible C–C loop.

Most interestingly from a functional point of view, the peptide mix presented a potent Kv1.3 blocking activity. Only one specific part, i.e. the core fragment of the ClTx chimer seems to be responsible for the observed Kv1.3 channel inhibitory activity. Because there are six different fragments, future experiments will reveal whether these fragments possess a different pharmacology or not. Nevertheless, this work has shown that it is possible to confer K^+ channel inhibitory properties on a chimer chlorotoxin molecule. These results may offer interesting possibilities for future protein design and engineering.

Acknowledgements

Maria L. Garcia kindly provided the Kv1.3 clone. Isabelle Huys is Research Assistant of the Flemish Fund for Scientific Research (FWO, Vlaanderen). We thank Prof. Liliane Schoofs, Elke Clynen and Dr. Rita Derua for mass determinations. This work was supported by the Fund for Scientific Research–Flanders (FWO, Vlaanderen) by Grant G.0124.03.

References

[1] J.A. DeBin, G.R. Strichartz, Toxicon 29 (1991) 1403.
[2] J.A. DeBin, J.E. Maggio, G.R. Strichartz, Am. J. Physiol. 264 (1993) C361.
[3] J. Tytgat, T. Debont, K. Rostoll, G.J. Muller, F. Verdonck, P. Daenens, J.J. van der Walt, L.D. Possani, FEBS Lett. 441 (1998) 387.
[4] N. Ullrich, G.Y. Gillespie, H. Sontheimer, NeuroReport 7 (1995) 343.
[5] N. Ullrich, H. Sontheimer, Am. J. Physiol. 270 (1996) C1511.
[6] N. Ullrich, H. Sontheimer, Am. J. Physiol. 273 (1997) C1290.
[7] N. Ullrich, A. Bordey, G.Y. Gillespie, H. Sontheimer, Neuroscience 83 (1998) 1161.
[8] L. Soroceanu, T.J. Manning Jr., H. Sontheimer, J. Neurosci. 19 (1999) 5942.
[9] G. Lippens, J. Najib, S.J. Wodak, A. Tartar, Biochemistry 34 (1995) 13.
[10] F. Bontems, C. Roumestand, B. Gilquin, A. Menez, F. Toma, Science 254 (1991) 1521.
[11] J. Tytgat, K.G. Chandy, M.L. Garcia, G.A. Gutman, M.F. Martin-Eauclaire, J.J. van der Walt, L.D. Possani, Trends Pharmacol. Sci. 20 (1999) 444.
[12] M.L. Garcia, M. Garcia-Calvo, P. Hidalgo, A. Lee, R. MacKinnon, Biochemistry 33 (1994) 6834.
[13] I. Huys, K. Dyason, E. Waelkens, F. Verdonck, J. van Zyl, J. du Plessis, G.J. Muller, J. van der Walt, E. Clynen, L. Schoofs, J. Tytgat, Eur. J. Biochem. 269 (2002) 1854.
[14] R. Swanson, J. Marshall, J.S. Smith, J.B. Williams, M.B. Boyle, K. Folander, C.J. Luneau, J. Antanavage, C. Oliva, S.A. Buhrow, et al., Neuron 4 (1990) 929.
[15] C. Vita, C. Roumestand, F. Toma, A. Menez, Proc. Natl. Acad. Sci. U.S.A. 92 (1995) 6404.
[16] E. Drakopoulou, S. Zinn-Justin, M. Guenneugues, B. Gilqin, A. Menez, C. Vita, J. Biol. Chem. 271 (1996) 11979.
[17] C. Vita, E. Drakopoulou, J. Vizzavona, S. Rochette, L. Martin, A. Menez, C. Roumestand, Y.S. Yang, L. Ylisastigui, A. Benjouad, J.C. Gluckman, Proc. Natl. Acad. Sci. U.S.A. 96 (1999) 13091.
[18] J.M. Sabatier, C. Lecomte, K. Mabrouk, H. Darbon, R. Oughideni, S. Canarelli, H. Rochat, M.F. Martin-Eauclaire, J. van Rietschoten, Biochemistry 35 (1996) 10641.
[19] Q. Zhu, S. Liang, L. Martin, S. Gasparini, A. Menez, C. Vita, Biochemistry 41 (2002) 11488.
[20] V. Calabro, J.M. Sabatier, E. Blanc, C. Lecomte, V. Van Rietschoten, H. Darbon, J. Pept. Res. 50 (1997) 39.
[21] E. Drakopoulou, J. Vizzavona, J. Neyton, V. Aniort, F. Bouet, H. Virelizier, A. Menez, C. Vita, Biochemistry 37 (1998) 1292.
[22] J.P. Flinn, R. Murphy, R.B. Johns, W.A. Kunze, J.A. Angus, Int. J. Pept. Protein Res. 45 (1995) 320.
[23] J.M. Bonmatin, J.L. Bonnat, X. Gallet, F. Vovelle, M. Ptak, J.M. Reichhart, J.A. Hoffmann, E. Keppi, M. Legrain, T. Achstetter, J. Biomol. NMR 2 (1992) 235.
[24] M. Bruix, M.A. Jimenez, J. Santoro, C. Gonzalez, F.J. Colilla, E. Mendez, M. Rico, Biochemistry 32 (1993) 715.
[25] J.E. Caldwell, F. Abildgaard, Z. Dzakula, D. Ming, G. Hellekant, J.L. Markley, Nat. Struct. Biol. 5 (1998) 427.
[26] F. Ceciliani, F. Bortolotti, E. Menegatti, S. Ronchi, P. Ascenzi, S. Palmieri, FEBS Lett. 342 (1994) 221.
[27] I. Huys, J. Tytgat, Eur. J. Neurosci. 17 (2003) 1786.